

High magnetic field study of charge melting in $\text{Bi}_{1/2}(\text{Sr}, \text{Ca})_{1/2}\text{MnO}_3$ perovskites: Unconventional behavior of bismuth charge ordered compounds

A. Kirste,¹ M. Goiran,² M. Respaud,³ J. Vanaken,⁴ J. M. Broto,³ H. Rakoto,² M. von Ortenberg,¹ C. Frontera,⁵ and J. L. García-Muñoz⁵

¹*Magnetotransport in Solids, Humboldt-University, Invalidenstrasse 110, D-10115 Berlin, Germany*

²*Laboratoire National des Champs Magnétiques Pulsés, 143 avenue de Rangueil, Boîte Postale 4245, F-31432 Toulouse Cedex-4, France*

³*Laboratoire de la Physique de la Matière Condensée, INSA, 135 avenue de Rangueil, F-31077 Toulouse Cedex-4, France*

⁴*Laboratorium voor Vaste Stof-fysica en Magnetisme, K.U. Leuven, Celestijnenlaan 200 D, B-3001 Heverlee, Belgium*

⁵*Institut de Ciència de Materials de Barcelona, CSIC, Campus Universitari de Bellaterra, E-08193 Bellaterra, Spain*

(Received 9 September 2002; revised manuscript received 6 November 2002; published 10 April 2003)

The stability of charge ordered phases of bismuth based $\text{Bi}_{0.5}\text{Ca}_{0.5}\text{MnO}_3$ and $\text{Bi}_{0.5}\text{Sr}_{0.5}\text{MnO}_3$ oxides is investigated by magnetization measurements in magnetic fields up to 130 T. Marked differences exist when comparing the critical fields $\mu_0 H_C$ found to induce a ferromagnetic state in $\text{Bi}_{0.5}\text{M}_{0.5}\text{MnO}_3$ ($M=\text{Ca}, \text{Sr}$) and $\text{Ln}_{0.5}\text{Ca}_{0.5}\text{MnO}_3$ (Ln -rare-earth) manganites. Bi oxides do not match the general $\mu_0 H_C$ - θ or $\mu_0 H_C$ - T_{CO} monotonous tendencies showed by the half-doped manganites having rare earths. From this comparison, we suggest the possibility that, at least in the case of $\text{Bi}_{0.5}\text{Sr}_{0.5}\text{MnO}_3$, the high-field ferromagnetic phase below 130 T could be insulating in nature.

DOI: 10.1103/PhysRevB.67.134413

PACS number(s): 75.25.+z, 71.45.Lr, 71.38.-k, 71.27.+a

I. INTRODUCTION

Rare-earth-based manganites ($\text{Ln}_{1-x}\text{M}_x\text{MnO}_3$, Ln = rare earth, M = alkaline earth) have been the subject of large interest during the last years. Their colossal magnetoresistance¹ (CMR) and charge order (CO) phenomena^{2,3} displayed by many of these compounds have focused the attention of numerous research works. CMR has been understood to come from the correlation between the alignment of Mn magnetic moments and the mobility of the e_g electrons. Although recent studies evidence that there are also other important ingredients such as phase separation, percolation, etc., it is now well established that in the range $\approx 0.25 \leq x \leq 0.5$ the ferromagnetic state in these compounds is metallic. Besides, CO is usually understood in a purely ionic picture: it is viewed as a spatially ordered distribution of $\text{Mn}^{3+}/\text{Mn}^{4+}$ ions in the lattice.³ This order is accompanied by orbital order (OO): an ordered occupation of the e_g ($d_{3z^2-y^2}$ or $d_{x^2-y^2}$) orbitals. It is generally accepted that the driving forces of the CO/OO phases formation are the minimization of both the Coulomb repulsion (when CO appears) and the strain energy, related with the strong Jahn-Teller deformations around Mn^{3+} ions. These terms compete with the kinetic-energy term of e_g electrons that favors the ferromagnetic-metallic phase. Beyond this simple ionic picture, a more realistic scenario for the CO state in manganites emerges from recent studies,⁴⁻⁶ which have reported the formation of ordered Zener polarons (ZP): each e_g electron becomes trapped in a Mn-O-Mn trio (with quite opened Mn-O-Mn bond angle) instead of in a single Mn ion.⁴ The two Mn ions involved in the trio conserve an intermediate valence state and are ferromagnetically coupled by the double exchange interaction induced by the shared e_g electron.⁴ According to this new scenario, the CO phase of manganites must be understood as an ordered phase of Zener polarons

(ZPO). Along this paper, we will use CO in the sense of ZPO. In addition, the correlation between the one electron bandwidth W and the transition temperature T_{CO} appears now well established. Both are sterically controlled by $\langle r_A \rangle$, the mean size of the A cations (Ln and M). Large values of $\langle r_A \rangle$, enlarged values of W , favor the mobility of e_g electrons, thus, reducing T_{CO} .

After the electronic localization, the particular ordering of ZP in the CO (or ZPO) phase gives rise at low temperatures to an antiferromagnetic (AFM) coupling between zig-zag chains of FM coupled Zener units.⁴ This leads to the appearance of the AFM-CE structure characteristic of CO manganites. The evolution of the Néel temperature (T_N), where this magnetic ordering appears displays small and wandering variations when changing the rare earth. Due to the dispersion in the determination of T_N and the small variations displayed when changing the rare earth, a clear dependence of T_N on $\langle r_A \rangle$, and/or on T_{CO} cannot be easily drawn. For instance, $T_N \approx 158$ K, 155 K, 165 K, and 150 K for $\text{Nd}_{0.5}\text{Sr}_{0.5}\text{MnO}_3$ ($\langle r_A \rangle = 1.185$ Å),⁷ $\text{La}_{0.5}\text{Ca}_{0.5}\text{MnO}_3$ ($\langle r_A \rangle = 1.140$ Å),³ $\text{Nd}_{0.5}\text{Ca}_{0.5}\text{MnO}_3$ ($\langle r_A \rangle = 1.115$ Å),⁸ and $\text{Tb}_{0.5}\text{Ca}_{0.5}\text{MnO}_3$ ($\langle r_A \rangle = 1.080$ Å),⁹ respectively.

The observation that AFM, charge, and orbital ordered states can be disrupted by the application of external magnetic fields has stimulated intense work aimed at examining the coupled structural, magnetic, and electronic transitions induced under field and its relation with the structural details in each of these compounds.¹⁰⁻¹⁴ In the magnetic-field-melting mechanism the induced polarization of the electronic spins competes with the trapping of the charges and favors their delocalization. Thus, the FM state induced by the magnetic field is strongly favored by the energy gain due to its metallicity. This is reflected in the fact that the strength of the field needed to break the AFM order is related to T_{CO} (and thus to $\langle r_A \rangle$):¹¹⁻¹⁴ very different fields are needed to break

AFM couplings of similar strength (without important variations of T_N for the different compounds).

Bismuth-based manganites ($\text{Bi}_{1-x}\text{M}_x\text{MnO}_3$ $\text{M}=\text{Ca}, \text{Sr}$) have been recently found to display quite different behavior.^{15–18} In fact, they do not follow the dependency of T_{CO} on $\langle r_A \rangle$ described above.¹⁶ The properties of bismuth oxides can depend on the behavior of the highly polarizable $6s^2$ lone pair of Bi^{3+} . Bi^{3+} ions have been found to push T_{CO} up to 525 K in $\text{Bi}_{0.5}\text{Sr}_{0.5}\text{MnO}_3$, while $\text{Bi}_{0.5}\text{Ca}_{0.5}\text{MnO}_3$ displays $T_{CO} \approx 325$ K. The extraordinary enhancement of T_{CO} in the former has been attributed to an orientation of the $6s^2$ lone pair toward a surrounding anion O^{2-} , which can produce a local distortion or even a hybridization between $6s$ -Bi orbitals and $2p$ -O orbitals.¹⁹ This hybridization would produce a local distortion and reduce the mobility of e_g electrons, thus favoring charge order. In fact, resistivity measurements have revealed that $\text{Bi}_{1-x}\text{Sr}_x\text{MnO}_3$ ($x=0.0, 0.1, 0.2, 0.3, 0.5,$ and 0.67) compounds present a very large resistivity and insulating behavior at least up to room temperature.²⁰ It is also worth mentioning that compounds with a small doping ($x=0.0, 0.1, 0.2$) show a FM ground state. Another example where the $6s^2$ lone pair is weakly screened is BiMnO_3 .^{21,22} In this compound, there are indications suggesting that the localized lone pair has some contribution from the O $2p$ states.²² Very different is the case of $\text{Bi}_{0.5}\text{Ca}_{0.5}\text{MnO}_3$ ($T_{CO} \approx 325$ K). The apparent size of Bi^{3+} ions is smaller ($\text{Bi}^{3+} = 1.16$ Å) than in the Sr case ($\text{Bi}^{3+} = 1.24$ Å).¹⁶ This is an indication of the $6s^2$ lone pair of Bi to be strongly screened^{15,16} in $\text{Bi}_{0.5}\text{Ca}_{0.5}\text{MnO}_3$.

In order to gain insight into the mechanisms that drive these differences between (i) bismuth-based and rare-earth-based manganites, and (ii) between different bismuth compounds, we have performed a magnetization study on $\text{Bi}_{0.5}\text{Sr}_{0.5}\text{MnO}_3$ and $\text{Bi}_{0.5}\text{Ca}_{0.5}\text{MnO}_3$ in very high field.

II. EXPERIMENTAL DETAILS

Polycrystalline samples of $\text{Bi}_{0.5}\text{M}_{0.5}\text{MnO}_3$ ($\text{M}=\text{Ca}, \text{Sr}$) have been prepared by standard solid-state reaction as has been previously reported.¹⁶ Neutron powder diffraction (NPD) patterns were collected at ILL (Grenoble, France) in the temperature interval $1.5 < T < 700$ K. Several diffractometers and wavelengths were used, D2B ($\lambda = 1.594$ Å), D20 ($\lambda = 2.42$ Å), and D1B ($\lambda = 2.52$ Å). Synchrotron powder x-ray-diffraction patterns were collected on BM16 ($\lambda = 0.4424$ Å) diffractometer of ESRF (Grenoble, France) between 170 and 700 K. Structural and magnetic parameters were refined by the Rietveld method using the program FULLPROF,²³ and have been reported in detail in previous works.^{15–17}

Magnetic measurements have been done on a commercial superconducting quantum interference device (quantum design) under an applied field of 1 T, between 5 and 600 K. From these measurements, as well as from NPD data, we have established T_{CO} and T_N for both compounds as has been reported elsewhere.¹⁷

Powdered samples with a volume of a few mm^3 were

investigated by compensated pickup coils in pulsed fields up to 150 T generated by the semidestructive single-turn coil technique. The advantage of this method, as compared to the fully destructive flux-compression technique, is having both up and down sweep of the magnetic field applicable for the experiment as well as the survival of the sample and the equipment inside the field-generating coil. The magnetic field is produced by a very fast discharge of a capacitor bank into a single-turn coil having a usable inner diameter and width of 15 mm. This coil size is preferred for magnetization measurements since it offers a good compromise between high peak field and sufficiently good field homogeneity around the coil center. Even higher fields in excess of 200 T can be produced within smaller single-turn coils. Details can be found in Ref. 24. Specially designed He-flow cryostats made of nonconducting materials in the vicinity of the single-turn coil are capable of cooling samples down to 5 K.

The magnetization was measured by the voltage induced in a well-compensated pickup coil system. We used compensation coils consisting of two partial coils in parallel configuration, each having 20–30 turns. They were produced by alternatively winding $70 \mu\text{m}$ Cu wire in opposite directions around two parallel cylinders having an identical diameter of 1.40 mm. This allows obtaining full area compensation ratios better than 10^{-3} for empty coils in a homogeneous field. This compensation ratio, however, may change in single-turn coil experiments so that the uncompensated background signal, which is typically proportional to the field derivative dH/dt , may have a time dependence different from dH/dt . Considering the transient and frequency response of the measuring system, the time delay in the magnetization signal was not larger than 10 ns. Together with the uncertainty of the field measurement, the maximum uncertainty for all magnetic field values was less than 2 T. In particular, for the field values of any two corresponding events in up and down sweep, the field readings have thus a maximum uncertainty of 2×2 T.

In order to suppress trigger noise and other unwanted interference to the measurement system, the whole system (including pickup coils, cables, and digitizers) is enclosed in an electromagnetic screen, which is necessarily implemented as a wire metal in the vicinity of the single-turn coil. A detailed description of the measurement system is given in Ref. 25.

III. RESULTS

Figure 1 shows the signal picked up by the coil during up and down sweep of the magnetic field for both $\text{Bi}_{0.5}\text{Sr}_{0.5}\text{MnO}_3$ and $\text{Bi}_{0.5}\text{Ca}_{0.5}\text{MnO}_3$. The AFM to FM transition induced by the field produces a large signal in the coil reflected as the appearance of a peak in Fig. 1. In Refs. 16 and 17, we reported the coexistence of CE and A-type phases with nearly identical $T_{CO/00}$ and T_N in the $\text{Bi}_{0.5}\text{Sr}_{0.5}\text{MnO}_3$ specimen. By comparing the integration of the large peaks in Fig. 1, we estimate that the whole $\text{Bi}_{0.5}\text{Sr}_{0.5}\text{MnO}_3$ sample becomes fully FM between 55 and 65 T (increasing the

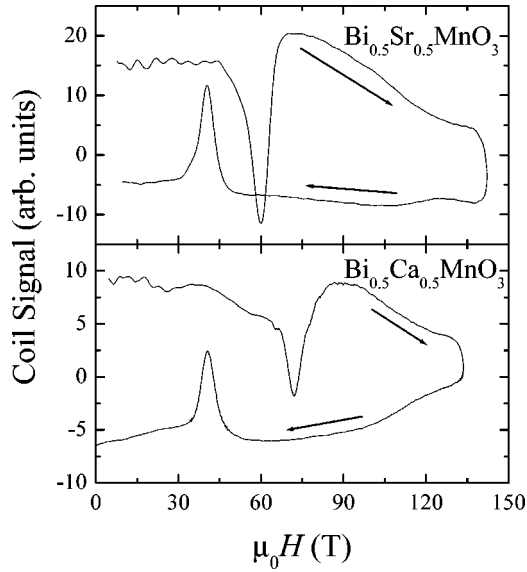


FIG. 1. Signal of the pickup coil for increasing and decreasing magnetic field for $\text{Bi}_{1/2}\text{M}_{1/2}\text{MnO}_3$ ($M=\text{Sr}, \text{Ca}$).

field). The transition in both samples presents, as usual, a high hysteresis between increasing and decreasing field. We define $\mu_0 H_C^+$ ($\mu_0 H_C^-$) as the field when the minimum (maximum) takes place for increasing (decreasing) field. The thermodynamic critical field ($\mu_0 H_C$) when the FM state is induced is defined as the average of these values: $(\mu_0 H_C^+ + \mu_0 H_C^-)/2$. From the peaks of Fig. 1, we have estimated that $\mu_0 H_C \approx 50$ T for $\text{Bi}_{0.5}\text{Sr}_{0.5}\text{MnO}_3$ and $\mu_0 H_C \approx 56$ T for $\text{Bi}_{0.5}\text{Ca}_{0.5}\text{MnO}_3$. Surprisingly, a stronger field is needed to induce the FM state in $\text{Bi}_{0.5}\text{Ca}_{0.5}\text{MnO}_3$ with its T_{CO} (325 K) being 200 K smaller than that of $\text{Bi}_{0.5}\text{Sr}_{0.5}\text{MnO}_3$ (525 K). From both NPD and magnetic measurements^{16,17} it can be concluded that Néel temperatures are very similar for both samples, although it is slightly smaller for $\text{Bi}_{0.5}\text{Sr}_{0.5}\text{MnO}_3$ ($T_N \approx 110$ K) than for $\text{Bi}_{0.5}\text{Ca}_{0.5}\text{MnO}_3$ ($T_N \approx 120$ K). The values of these Néel temperatures together with CO temperatures, the values of $\mu_0 H_C^+$, $\mu_0 H_C^-$, $\mu_0 H_C$, and average Mn-O-Mn bond angle for both compounds are summarized in Table I.

Figure 2(a) shows the dependence of $\mu_0 H_C$ on the average Mn-O-Mn bond angle for different rare-earth-based manganites half doped with Ca (Ref. 14) compared with those obtained from Fig. 1. It must be highlighted that neither $\text{Bi}_{0.5}\text{Sr}_{0.5}\text{MnO}_3$ nor $\text{Bi}_{0.5}\text{Ca}_{0.5}\text{MnO}_3$ match the general tendency displayed by rare-earth-based half-doped manganites. Figure 2(b) shows the same values plotted versus T_{CO} . The evolution of $\mu_0 H_C$ for the rare-earth compounds included in Fig. 2 has been discussed in detail in previous

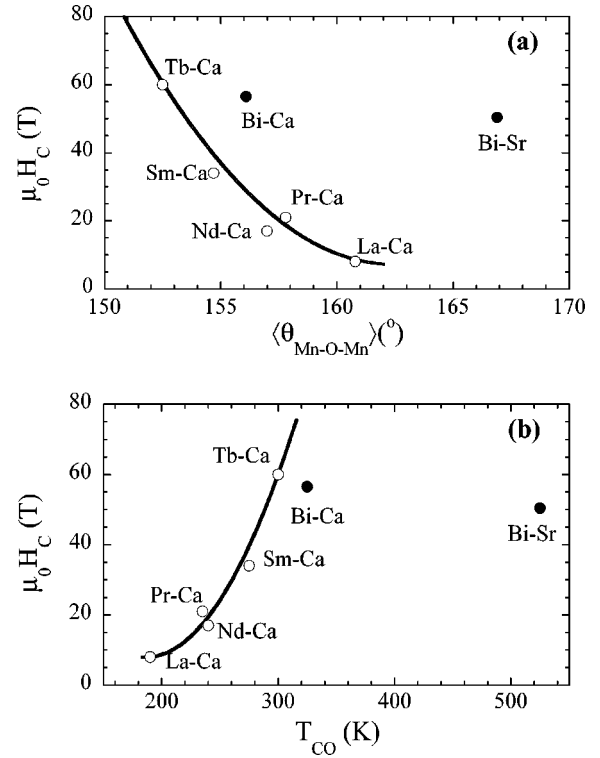


FIG. 2. Critical magnetic fields for several rare-earth-based manganites half doped with Ca (open symbols) together with those of $\text{Bi}_{0.5}\text{Sr}_{0.5}\text{MnO}_3$ and $\text{Bi}_{0.5}\text{Ca}_{0.5}\text{MnO}_3$ (filled symbols), plotted as function of Mn-O-Mn bond angle (a) and as function of T_{CO} (b). The lines are, in both panels, guides to the eyes.

works.^{10–14} From Fig. 2(a) $\text{Bi}_{0.5}\text{Ca}_{0.5}\text{MnO}_3$ and $\text{Bi}_{0.5}\text{Sr}_{0.5}\text{MnO}_3$ exhibit critical fields drastically larger than the values that one could expect from the dependency of $\mu_0 H_C$ on the mean Mn-O-Mn bond angle obtained for the $\text{Ln}_{0.5}\text{Ca}_{0.5}\text{MnO}_3$ family. On the contrary, from Fig. 2(b), both $\text{Bi}_{0.5}\text{Sr}_{0.5}\text{MnO}_3$ and $\text{Bi}_{0.5}\text{Ca}_{0.5}\text{MnO}_3$ present a critical field smaller than the corresponding according to their T_{CO} . The deviation from the general tendency is moderated for $\text{Bi}_{0.5}\text{Ca}_{0.5}\text{MnO}_3$, but it is very important for $\text{Bi}_{0.5}\text{Sr}_{0.5}\text{MnO}_3$.

IV. DISCUSSION

The results shown in the preceding section reveal remarkable differences when comparing not only bismuth and rare-earth half-doped perovskites, but also, respectively, bismuth-based Sr and Ca doped manganites. Next, we will show that a key factor in all cases is the highly polarizable $6s^2$ lone pair of Bi. The melting under field of the CO phase in half-doped rare-earth-based manganites has to be reinterpreted

TABLE I. Average Mn-O-Mn bond angles, critical fields, CO temperatures, and Néel temperatures of $\text{Bi}_{0.5}\text{Sr}_{0.5}\text{MnO}_3$ and $\text{Bi}_{0.5}\text{Ca}_{0.5}\text{MnO}_3$.

	$\langle \theta \rangle (^\circ)$	$\mu_0 H_C^+$ (T)	$\mu_0 H_C^-$ (T)	$\mu_0 H_C$ (T)	T_{CO} (K)	T_N (K)
$\text{Bi}_{1/2}\text{Ca}_{1/2}$	156.1(1)	72	40	56	325	120
$\text{Bi}_{1/2}\text{Sr}_{1/2}$	166.9(5)	60	40	50	525	110

within the new framework for the CO phenomena proposed by Daoud-Aladine *et al.* in Ref. 4. We recall here that in the new scenario the ordering of $\text{Mn}^{3+}/\text{Mn}^{4+}$ ions (ionic picture) has been substituted by the ordering of Zener polarons. Thus, a key factor is the fact that the e_g electron trapped in each ZP is shared by the two Mn ions involved. Consequently, the two Mn in the Mn-O-Mn trio are ferromagnetically coupled by the double exchange interaction (intermediate valence state). This situation is qualitatively different to having a pair of $\text{Mn}^{3+}/\text{Mn}^{4+}$ ions coupled ferromagnetically due to superexchange (ionic picture). According to Ref. 4, at low-temperatures superexchange exclusively applies to the coupling between different ZP's: FM coupled along zig-zag chains and AFM between them. As a consequence, the double exchange nature of the local FM coupling between Mn within the ZP (in the ZPO model) is probably responsible for the moderate stability of the ZPO phase against the application of magnetic fields (few tesla). A contradiction of the ionic picture was that a higher stability than that experimentally observed was expected for an ordered crystal of $\text{Mn}^{3+}/\text{Mn}^{4+}$ ions. At variance, in the case of ordered ZP, the CO phase contains very small FM clusters (two Mn atoms) than would act as the FM seed from which large FM clusters can develop under application of an external magnetic field. On another hand, the field needed to melt the lattice of ZP in half-doped manganites is mainly determined by structural features. These steric properties govern the kinetic-energy gain when the metallic (and FM) phase is induced by the field: the larger this energy gain, the smaller T_{CO} and $\mu_0 H_C$.

Remarkably, we have found that the field necessary to induce a FM state is slightly smaller for $\text{Bi}_{0.5}\text{Sr}_{0.5}\text{MnO}_3$ than for $\text{Bi}_{0.5}\text{Ca}_{0.5}\text{MnO}_3$, even when T_{CO} of the former is about 200 K larger than that of the latter. At the same time $\mu_0 H_C$ for both compounds are much larger (specially in the case of Bi-Sr) than the value expected for their average Mn-O-Mn bond angles. Even when they present Néel temperatures significantly smaller (30–40 K lower) than the rare-earth-based manganites. It is clear that the stability under field of Bi compounds do not follow the same general tendency than those of $\text{Ln}_{0.5}\text{Ca}_{0.5}\text{MnO}_3$ compounds. In the case of $\text{Bi}_{0.5}\text{Sr}_{0.5}\text{MnO}_3$ the difference is very important although for $\text{Bi}_{0.5}\text{Ca}_{0.5}\text{MnO}_3$ it is much less significant.

Given that $\text{Bi}_{0.5}\text{Sr}_{0.5}\text{MnO}_3$ falls completely out of the general tendency displayed by the half-doped rare-earth compounds, in our opinion, this can be an indication that the nature of the field-induced phase in this compound is markedly different from the FM metallic state induced in Ln-based compounds. The evidence is not so strong for $\text{Bi}_{0.5}\text{Ca}_{0.5}\text{MnO}_3$ (we recall that in any case Bi^{3+} is a very electronegative ion compared with the rare earths). We suggest that in the case of $\text{Bi}_{0.5}\text{Sr}_{0.5}\text{MnO}_3$ the main difference in the final (high field) state may concern its metallicity. Namely, in the field-induced state of $\text{Bi}_{0.5}\text{Sr}_{0.5}\text{MnO}_3$ the charges could be localized, this state being comparable to the FM insulating state reported for BiMnO_3 .²¹ In the present case, however, this possible interpretation would imply that the ZPO is not melted by the magnetic field (at least up to the highest field in our measurements, 135 T), and the *meta-*

magnetic transition found in Fig. 1 would correspond to the disruption of the CE-type AFM structure due to the FM alignment of Mn moments, with only the magnetic coupling term being involved in the transition. Furthermore, if this possibility for the final FM state of $\text{Bi}_{0.5}\text{Sr}_{0.5}\text{MnO}_3$ were true as well for $\text{Bi}_{0.5}\text{Ca}_{0.5}\text{MnO}_3$ (final FM insulating state), this would easily explain why the critical field of $\text{Bi}_{0.5}\text{Sr}_{0.5}\text{MnO}_3$, with $T_N \approx 110$ K, is smaller than that of $\text{Bi}_{0.5}\text{Ca}_{0.5}\text{MnO}_3$, with $T_N \approx 120$ K.

V. CONCLUSIONS

We have investigated the stability under magnetic field of charge ordered phases of half-doped bismuth-based manganites $\text{Bi}_{0.5}\text{Ca}_{0.5}\text{MnO}_3$ and $\text{Bi}_{0.5}\text{Sr}_{0.5}\text{MnO}_3$, the last having the highest T_{CO} reported in manganese oxides. In two very well characterized samples, low-temperature magnetization measurements were performed in very high magnetic fields up to 130 T. Field-induced transitions giving ferromagnetic phases were observed at high critical fields ($\mu_0 H_C \approx 50$ T for $\text{Bi}_{0.5}\text{Sr}_{0.5}\text{MnO}_3$ and $\mu_0 H_C \approx 56$ T for $\text{Bi}_{0.5}\text{Ca}_{0.5}\text{MnO}_3$). We remark that these values of $\mu_0 H_C$ found are much larger than one would expect from their Mn-O-Mn bond angles. None of both match the general $\mu_0 H_C - \theta$ or $\mu_0 H_C - T_{CO}$ tendencies showed by the half-doped manganites having rare earths. The differences are remarkably important for $\text{Bi}_{0.5}\text{Sr}_{0.5}\text{MnO}_3$, and for $\text{Bi}_{0.5}\text{Ca}_{0.5}\text{MnO}_3$ are much less significant. Surprisingly, a stronger field is needed to induce a FM state in $\text{Bi}_{0.5}\text{Ca}_{0.5}\text{MnO}_3$ than in $\text{Bi}_{0.5}\text{Sr}_{0.5}\text{MnO}_3$, despite T_{CO} for the former (Ca, 325 K) is 200 K smaller than for the latter (Sr, 525 K).

Of special relevance is the case of $\text{Bi}_{0.5}\text{Sr}_{0.5}\text{MnO}_3$ with a quite opened Mn-O-Mn bond angle. As happens with their CO temperature, this angle does not govern the field needed to induce FM moments in the compound. The possibility that the nature of the FM-field-induced state in $\text{Bi}_{0.5}(\text{Sr},\text{Ca})_{0.5}\text{MnO}_3$ compounds could be different from that of $\text{Ln}_{0.5}\text{Ca}_{0.5}\text{MnO}_3$ ones (at least for $\text{Bi}_{0.5}\text{Sr}_{0.5}\text{MnO}_3$) cannot be ruled out. Thus, it is not clear at present whether in $\text{Bi}_{0.5}\text{Sr}_{0.5}\text{MnO}_3$ (and perhaps $\text{Bi}_{0.5}\text{Ca}_{0.5}\text{MnO}_3$) the field below 135 T is really melting the CO (ZPO) phase or just breaking the AFM coupling between the FM zig-zag chains of localized ZP. In the latter case, the extension of the mobility region of the e_g electron will remain unchanged and the induced FM phase would be insulating rather than metallic. This, when examining the Néel temperatures ($T_N \approx 110$ K for Sr and 120 K for Ca), could also explain why the critical field is smaller for $\text{Bi}_{0.5}\text{Sr}_{0.5}\text{MnO}_3$ than for $\text{Bi}_{0.5}\text{Ca}_{0.5}\text{MnO}_3$.

ACKNOWLEDGMENTS

Financial support by the MEC (Grant No. PB97-1175), CICYT (Grant No. MAT99-0984-C03-01), and Generalitat de Catalunya (Grant Nos. GRQ95-8029 and PICS2001-22) is thanked. C.F. acknowledges financial support from MCyT. We also acknowledge the High Field Infrastructure Cooperative Network (Grant No. HPRI-1999-CT-0013) for financial support.

- ¹S. Jin, T.H. Tiefel, M. McCormack, R.A. Fastnacht, R. Ramesh, and L.H. Chen, *Science* **264**, 413 (1994).
- ²J.B. Goodenough, *Phys. Rev.* **100**, 564 (1955).
- ³P. Radaelli, D. Cox, M. Marezio, and S.-W. Cheong, *Phys. Rev. B* **55**, 3015 (1997).
- ⁴A. Daoud-Aladine, J. Rodríguez-Carvajal, L. Pinsard-Gaudart, M.T. Fernández-Díaz, and A. Revcolevschi, *Phys. Rev. Lett.* **89**, 097205 (2002).
- ⁵J. Rodríguez-Carvajal, A. Daoud-Aladine, L. Pinsard-Gaudart, M.T. Fernández-Díaz, and A. Revcolevschi, *Physica B* **320**, 1 (2002).
- ⁶A. Daoud-Aladine, J. Rodríguez-Carvajal, L. Pinsard-Gaudart, M.T. Fernández-Díaz, and A. Revcolevschi, *Appl. Phys. A: Mater. Sci. Process.* **A74**, s1758 (2002).
- ⁷P.M. Woodward, D.E. Cox, T. Vogt, C.N.R. Rao, and A.K. Cheetham, *Chem. Mater.* **11**, 3528 (1999).
- ⁸C. Frontera, J.L. García-Muñoz, A. Llobet, C. Ritter, J.A. Alonso, and J. Rodríguez-Carvajal, *Phys. Rev. B* **62**, 3002 (2000).
- ⁹J. Blasco, C. Ritter, J. García, J.M. de Teresa, J. Pérez-Cacho, and M.R. Ibarra, *Phys. Rev. B* **62**, 5609 (2000).
- ¹⁰Y. Tomioka, A. Asamitsu, Y. Moritomo, H. Kuwahara, and Y. Tokura, *Phys. Rev. Lett.* **74**, 5108 (1995); Y. Tomioka, A. Asamitsu, H. Kuwahara, Y. Moritomo, and Y. Tokura, *Phys. Rev. B* **53**, R1689 (1996).
- ¹¹Y. Tokura, H. Kuwahara, Y. Moritomo, Y. Tomioka, and A. Asamitsu, *Phys. Rev. Lett.* **76**, 3184 (1996); H. Kuwahara, Y. Tomioka, A. Asamitsu, Y. Moritomo, and Y. Tokura, *Science* **270**, 961 (1995).
- ¹²H. Kuwahara, Y. Moritomo, Y. Tomioka, A. Asamitsu, M. Kasai, R. Kumai, and Y. Tokura, *Phys. Rev. B* **56**, 9386 (1997).
- ¹³M. Tokunaga, N. Miura, Y. Tomioka, and Y. Tokura, *Phys. Rev. B* **57**, 5259 (1998).
- ¹⁴M. Respaud, A. Llobet, C. Frontera, C. Ritter, J.M. Broto, H. Rakoto, M. Goiran, C. Ritter, and J.L. García-Muñoz, *Phys. Rev. B* **61**, 9014 (2000), and references therein.
- ¹⁵C. Frontera, J.L. García-Muñoz, A. Llobet, M.A.G. Aranda, C. Ritter, M. Respaud, and J. Vanacken, *J. Phys.: Condens. Matter* **13**, 1071 (2001).
- ¹⁶J.L. García-Muñoz, C. Frontera, M.A.G. Aranda, A. Llobet, and C. Ritter, *Phys. Rev. B* **63**, 064415 (2001).
- ¹⁷C. Frontera, J.L. García-Muñoz, M.A.G. Aranda, A. Llobet, C. Ritter, M. Respaud, and J. Vanacken, *Phys. Rev. B* **64**, 054401 (2001).
- ¹⁸M. Hervieu, A. Maignan, C. Martin, N. Nguyen, and B. Raveau, *Chem. Mater.* **13**, 1356 (2001).
- ¹⁹N.A. Hill and K.M. Rabe, *Phys. Rev. B* **59**, 8759 (1999).
- ²⁰H. Chiba, T. Atou, and Y. Syono, *J. Solid State Chem.* **132**, 139 (1997).
- ²¹T. Atou, H. Chiba, K. Ohoyama, Y. Yamaguchi, and Y. Syono, *J. Solid State Chem.* **145**, 639 (1999).
- ²²R. Seshadri and N.A. Hill, *Chem. Mater.* **13**, 2892 (2001).
- ²³J. Rodríguez-Carvajal, *Physica B* **192**, 55 (1993).
- ²⁴O. Portugall, N. Puhlmann, H.U. Müller, M. Barczewski, I. Stolpe, and M. von Ortenberg, *J. Phys. D* **32**, 2354 (1999).
- ²⁵A. KIRSTE, N. Puhlmann, I. Stolpe, H.-U. Mueller, M. von Ortenberg, O.M. Tatsenko, V. Platonov, Z.A. Kazei, N.P. Kolmakova, and A.A. Sidorenko, *Physica B* **294-295**, 132 (2001).